Journal of Molecular Neuroscience (2021) 71:638–650
https://doi.org/10.1007/s12031-020-01685-7

# The Effect of Optogenetic Inhibition of the Anterior Cingulate Cortex in Neuropathic Pain Following Sciatic Nerve Injury

K. C. Elina[1] · Hyeong Cheol Moon[1,2] · Jaisan Islam[1] · Hyong Kyu Kim[3] · Young Seok Park[1,2]

Received: 8 May 2020 / Accepted: 11 August 2020 / Published online: 18 August 2020


## Abstract

Cortical disinhibition is the underlying pathological alteration contributing to neuropathic pain associated with peripheral nerve injury. Nerve injury resulting in disinhibition of the anterior cingulate cortex has been reported. However, the effect of optogenetic inhibition of the anterior cingulate cortex (ACC) on the sensory component of nerve injury–induced neuropathic pain has not been well studied. To investigate the feasibility of optogenetic ACC modulation, we injected an optogenetic virus or a null virus into the ACC of a nerve injury–induced neuropathic pain model. The unilateral ACC was modulated, and the optogenetic effect was measured by mechanical and thermal sensitivity tests. The assessment was performed in "pre—light off," "stimulation—yellow light on," and "post—light off" states. Optogenetic inhibition of the ACC in injury models revealed improved mechanical and thermal latencies with profound pain-relieving effects against nerve injury–induced neuropathic pain. The sensory thalamic discharge in electrophysiological in vivo recordings was also altered during laser stimulation. This finding indicates that hyperactivity of the ACC in nerve injury increases output to the spinothalamic tract through direct or indirect pathways. The direct photoinhibition of ACC neurons could play a vital role in restoring equilibrium and provide novel insight into techniques that can assuage peripheral nerve injury–induced neuropathic pain.

**Keywords** Anterior cingulate cortex · Neuropathic pain · Neural circuitry · Optogenetics · Thalamus

## Introduction

Chronic neuropathic pain resulting from peripheral nerve injury (PNI) is a significant clinical problem that often proves refractory to current treatments and is the foremost cause of disability (Dodla et al. 2019). The anterior cingulate cortex (ACC), a cortical structure in the brain, is known for its prominent role in facilitating emotional and attentive pain responses. Increasing evidence via human neuroimaging studies (Osaka et al. 2004; Hsieh et al. 1999; Hutchison et al. 1999; Xiao et al. 2019) and other animal model studies (Nazeri et al. 2019) suggests the role of the ACC in mediating the sensational component of physiological and pathological pain as well. Pharmacological studies of electrical stimulation have suggested the role of ACC in pain regulation (Fuchs et al. 2014a; LaGraize et al. 2004; Zhuo 2014a). In vivo characterization of pain-related L5 pyramidal ACC neuronal activity in awake mice has also demonstrated that the development of neuropathic pain is accompanied by elevated spontaneous and evoked neuronal activity in the ACC (Zhao et al. 2018). Pyramidal neurons in the ACC are one of the important mediators of pain perception. A previous report stated the effect of ACC glutamatergic synaptic plasticity in persistent pain via extracellular signal–regulated kinase (Erk) activation (Wei and Zhuo 2008). Furthermore, studies have also shown that the alteration in intrinsic excitability in L5 pyramidal neurons and the loss of local bidirectional connections between pyramidal cells and fast-spiking interneurons of the anterior cingulate cortex results in cortical disinhibition (Blom et al. 2014a). In peripheral nerve–injured animals, these effects on synaptic tone autoregulation (Tachibana et al. 2008; Zhuo 2006) might lead to ACC pyramidal neuron overexcitation.

**Electronic supplementary material** The online version of this article (https://doi.org/10.1007/s12031-020-01685-7) contains supplementary material, which is available to authorized users.

✉ Young Seok Park
youngseokparkmd@gmail.com

[1] Department of Neuroscience, College of Medicine, Chungbuk National University, Cheongju, South Korea

[2] Department of Neurosurgery, Chungbuk National University Hospital, 776, 1 Sunhwanro, Seowon-gu, Cheongju-Si, Chungbuk 28644, South Korea

[3] Department of Medical and Microbiology, College of Medicine, Cheongju, South Korea

Moreover, the T-type calcium channel may upregulate ACC neuronal activity in a neuropathic animal pain model (Jagodic et al. 2008; Shen et al. 2015), which suggests that inhibiting the activity of this region may assuage pain.

An optogenetic approach to the management of neuropathic pain enables the definition of the expression of engineered opsins in non–light sensitive cells, allowing rapid activation and silencing and thus providing better insight into pain pathways (Daou et al. 2013; Lee and Kim 2016; Zachariou and Carr 2014). Among many isoforms, halorhodopsin from *Natronomonas phraraonis* (NpHR) has been extensively used to inhibit action potentials or hyperpolarization in cells by extracellular chloride influx (Gradinaru et al. 2008). Currently, three generations of NpHRs are available. eNpHR3.0, a yellow light–sensitive enhanced third-generation chloride pump halorhodopsin NpHR, is the most stable with longer time scales (Liu et al. 2019) and has been successfully used to prevent pain in a neuropathic pain model in vivo (Iyer et al. 2016).

The functional association between the medial thalamus and ACC has been studied, suggesting the involvement of the medial thalamus in the affective–motivational component of pain (Harte et al. 2011). Zhao et al. found that PNI induces alternations in sodium channel expression within ventral posterolateral (VPL) thalamic neurons and increases neuronal excitability, contributing to neuropathic pain (Zhao et al. 2006). However, the functional association between the ACC and the VPL thalamus has not yet been studied. Thus, regarding the roles of the ACC and the VPL thalamus in PNI, we sought to investigate the feasibility of optogenetic inhibition of ACC neurons with eNpHR3.0 in a chronic constriction injury (CCI) rat model. In addition, we tested whether this inhibition modulates the firing activity of VPL thalamic neurons.

## Materials and Methods

Adult female Sprague Dawley rats (200–230 g; Koatech, Pyeongtaek, South Korea) were used in the study and kept under normal laboratory conditions (temperature, 22 °C; humidity, 30%; 12/12-h light-dark cycle) in a conventional area. The rats were allowed free access to commercial food and water (McCutcheon et al. 2014) and were housed in separate cages in a randomized manner. Animal experiments were performed according to the national guidelines and with approval from the Institutional Animal Care Committee of Chungbuk National University (CBNUR-1072-17). All experiments were conducted inside the Laboratory Animal Research Center, Chungbuk National University, in agreement with the proper regulations of the International Association for the Study of Pain (Zimmermann 1986). The experimental timeline is shown in Supplementary Figure 1a.

### Sciatic Nerve Constriction Injury Model

The rats were randomly assigned to the sham-treated or CCI groups. A combination of 15-mg/kg Zoletil50® (tiletamine/zolazepam; Virbac Laboratories, Carros, France) and 9-mg/kg Rompun® (xylazine; Bayer AG, Leverkusen, Germany) in saline was used for anesthesia purposes. The rats underwent sciatic nerve chronic constriction surgeries to create PNI-induced neuropathic pain on the right hind limb under anesthesia. We followed the surgical protocol discussed in previous studies (Bennett and Xie 1988; De Vry et al. 2004; Xu et al. 2018). Briefly, the right sciatic nerve was exposed under sterile conditions after trimming the surrounding tissues with micro scissors 10 mm distal to the sciatic notch. Two silk suture ligatures were made loosely with approximately 1-mm gaps (Supplementary Figure 1b), and the incision was fastened in layers with skin sutures. In sham-treated controls, similar surgical tactics were used on the same side under identical anesthetic circumstances short of the sciatic nerve ligation. None of the animals received postoperative analgesics.

### Stereotaxic Virus Injection

Simultaneously, with sciatic constriction or sham surgery, an adeno-associated viral (AAV) vector carrying human synapsin1 (hSyn)-eNpHR3.0EYFP or EYFP alone (null virus) was injected unilaterally into the left ACC (coordinates from bregma: anterior–posterior (AP) = + 2.6 mm; medial–lateral (ML) = − 0.6 mm; dorsal–ventral (DV) = − 2.8 mm) with 10-μl Hamilton syringe directed by syringe pump (Legato® 130, KD Scientific, USA) at the flow rate of 0.4 μl/min for 5 min (Supplementary Figure 1c). The viral vectors were purchased from the Korea Institute of Science and Technology (Seoul, South Korea). After injection, the syringe was kept in place for 10 min to avert backflow. The concentrations of optogenetic and null viruses were 2.23 × 1013 GC/ml and 1.9 × 1013 GC/ml, respectively. Based on virus injection and surgery type, rats were further divided into four groups: (i) CCI/NpHR+, which received the optogenetic virus and CCI surgery; (ii) CCI/NpHR−, which received the null virus and CCI surgery; (iii) sham+NpHR+, which received the optogenetic virus and sham surgery; and (iv) sham+NpHR−, which received the null virus and sham surgery. Due to the superior biosafety rating, low immunogenicity, and long-term expression of exogenous genes, AAV is an ideal gene therapy vector in vivo (Shevtsova et al. 2005). The hSyn promoter is useful for quantifying neuronal populations (both excitatory

and inhibitory neurons) from glia and other cells (Kügler et al. 2003). We used hSyn to preferentially express the optogenetic construct in neurons.

## Optical Fiber Implantation

Three weeks after optogenetic/null virus injection, a mono fiber-optic cannula (200-μm core, 230-μm outer diameter, numerical aperture of 0.48, MFC_200/230-0.48_###_ZF2.5_A45, Doric Lenses; Québec City, Québec, Canada) was surgically implanted under anesthesia at the left ACC. The optic cannula was inserted 2.5-mm deep from the skull surface mm and was securely fixed in place with superbond followed by dental cement (Ortho-ject Pound Package, Lang Dental, USA).

## Mechanical and Thermal Sensitivity Tests

A baseline behavior test was performed prior to surgery but after habituation. On the 1st, 7th, 14th, and 21st days post-surgery, mechanical and thermal sensitivity tests were performed (Nirogi et al. 2012). To measure hyperalgesia, we used the dynamic plantar aesthesiometer (model 37450; Ugo Basile, Italy) and Peltier plate (hot/cold plate, Ugo Basile, Italy). Rats were positioned in plexiglas cages (20 × 20 × 14 cm) with a grid bottom and kept for habituation for at least 30 min. Mechanical stimuli were performed by a metal filament to the hind paw with increasing pressure (0 to 50 g) on the plantar region of the ipsilateral and contralateral hind paws. A maximal cutoff threshold was set to 50 g to prevent tissue damage (Kim et al. 2015). Mechanical pain sensitivity was measured as the mechanical hind paw withdrawal threshold (PWT) and paw withdrawal latency (PWL). Each value represents the mean of three measurements.

For the thermal sensitivity test, rats were placed on a temperature-controlled plate set to 50 °C, and nociceptive behaviors such as bouncing or licking the hind paw were recorded as a response (Cai et al. 2014; Deuis and Vetter 2016; Kim et al. 2014). The mean was calculated using three assessments performed on a day.

## Optical Inhibition

A continuous yellow laser with a 589-nm wavelength resulted in activation of the eNpHR3.0 ion channel (Moon et al. 2017). A behavioral test under optical modulation was performed after 1 week of recovery. Yellow laser light (model: YL589T3-010FC, 589-nm yellow DPSS laser with fiber coupled (T3), Shanghai Laser & Optics Century Co., Ltd., Shanghai, China) was delivered through a monofiber optic patch chord to the optic cannula implant in ACC. The laser parameters were adjusted by using a waveform generator (33511B, Keysight Technologies, Santa Rosa, CA, USA) that allowed control of the frequency, pulse square, and pulse width. The yellow light stimulation parameters were a frequency of 20 Hz, pulse width of 50 nm, and tip laser intensity of 10 mw/mm$^2$ (Chiou et al. 2016; Kang et al. 2015b). As mentioned above, mechanical and thermal pain sensitivity tests were assessed under three conditions: before the laser was turned on (pre), while the laser was on (stim), and after the laser was turned off (post). Optic inhibition was performed with continuous light for 5 min, and each condition was assessed thrice. The mean value was taken as the final count.

## Single-Unit Extracellular Recording

Sham rats and those with CCI underwent extracellular single-unit recording from VPL thalamic neurons according to established methods (Huh et al. 2012; KC et al. 2020; Zhao et al. 2006). The same anesthesia combination was used as before. The head of each rat was fixed on a stereotaxic frame kept inside the Faraday enclosure. A small cranial window was prepared just above the ventral posterolateral nucleus (AP: − 3.2 mm; ML: + 1.5 mm; DV: − 6.0 mm), and in vivo extracellular recordings were made with a (Liu et al. 2015) quartz-insulated carbon electrode (E1011, Carbostar-1, Kation Scientific, Minneapolis, MN, USA). We acquired neural cell signals with a digital high-density electrophysiology acquisition system (Digital Lynx 4SX, Neuralynx Inc., Bozeman, MT, USA), and then, signals were amplified and digitized (sampling rate: 32 kHz, filtered at 0.9–6 kHz). The recorded individual activity was retrieved and analyzed offline using the SpikeSort 3D software (Neuralynx Inc., Bozeman, MT, USA). Neuronal discharge was evaluated in the contralateral VPL thalamus of lesioned and sham animals. The rate histograms (spike/s) of lesioned animals under different optical conditions were analyzed. Activity in the thalamic neurons was split up into burst rates (bursts per second) and mean firing rates (spikes per second) in each optical stimulation condition using NeuroExplorer version 4 (NEXTechnologies, CO, 80906, USA). Activity was assessed for 5 min in each state (pre, stim, and post). We defined burst rates as a group of at least three spikes with a maximum interval of 4 ms between spikes and an interval of 100 ms between bursts. We selected similar interspike interval histograms for comparison among the groups.

## Immunofluorescence

The rats were anesthetized with the previously mentioned anesthetic combination and transcardially perfused (Gage et al. 2012) with phosphate buffer solution (PBS) followed by 4% paraformaldehyde (PFA), and the brains were extracted after decapitation (Leica Biosystems, Buffalo, USA). The brains were fixed overnight in 4% PFA, followed by dehydration in 30% sucrose until the brain samples completely sank. The

samples were embedded and frozen with optimal cutting temperature (OCT) compound (Tissue Tek, Leica, USA), isopentane, and liquid nitrogen. A cryostat (Thermo Scientific, Waltham, MA, USA) was used to cut coronal sections of the brain (25 μm). Then, slides were immersed in chilled acetone solution and subsequently washed with PBS for 10 min. Tissue sections were blocked with TBST containing normal goat serum (NGS) at room temperature for 1 h. The sections were incubated with the primary antibody anti-c-fos (1:500, ab209794, Abcam) diluted in TBST with NGS overnight at 4 °C. Sections were then washed in PBS and incubated with Alexa Fluor 488 (ab150077, Abcam) in NGS in TBST at room temperature for 2 h. The sections were rinsed in PBS, and antifade mounting medium with DAPI (Vectashield®, Vector Laboratories, Inc. Burlingame, CA 94010) (Im et al. 2019) was added to slide followed by coverslip. Fluorescence microscopy and the cellSens Standard (Olympus Corp., Tokyo, Japan) software were used to capture the expression in the target area. The ImageJ software (National Institutes of Health, Bethesda, MD, USA) was used to merge the images and quantification of c-fos and eyfp. Transfection efficiency of AAV virus was calculated using the following formula:

Transfection efficiency (%) = (number of cells stained with fluorescent positive control dye/total number of cells per field) × 100.

### Statistical Analysis

All data analysis was performed using GraphPad Prism (GraphPad Software version 8.4.2, Inc., San Diego, CA, USA) and presented as the mean ± standard deviation (SD). We performed an unpaired *t* test and ordinary one- or two-way analysis of variance (ANOVA) with Tukey's post hoc multiple comparisons test depending on the experimental conditions. $*p < 0.05$ was considered statistically significant in all cases. Behavioral tests were calculated from the mean rates for each of the optical conditions. Unpaired *t* tests were used to compare firing rates between CCI and sham-operated animals. Quantification of c-fos was performed using the ImageJ software.

## Results

The delivery of AAV-hSyn-eNpHR3.0-EYFP and AAV-hSyn-EYFP ensured reliable virus transfection and colocalization in the ACC. We used optogenetics to inhibit ACC excitatory neurons to investigate the role of the ACC in sensory neuropathic pain. Three weeks following virus injection, viral expression was observed in the ACC (Fig. 1). We observed the expression of c-fos immunoreactivity, a neuronal marker, to confirm functional eNpHR. We found that the CCI rats showed increased c-fos expression in the ACC region of the NpHR group compared with that of the sham rats receiving EYFP alone. We found insignificant differences in transfection efficiency of AAV virus among the four groups (Fig. 1 and Supplementary Figure 2). This result agrees with previous findings that the cognition of pain and typical neuropathic characteristics such as allodynia activate the ACC (Sugimine et al. 2016).

### Changes in Pain Behaviors Following Sciatic Nerve Constriction

Sciatic nerve constriction injury gradually increased mechanical and thermal sensitivity over 14 days compared with the sensitivity experienced by the sham group. The PWT is the maximum weight withheld by the pricked paw. The PWT of the ipsilateral or right hind paw in CCI rats showed significant differences from 36.075 ± 5.09 to 12.98 ± 3.22 g compared with that of sham controls that had values ranging from 35.20 ± 2.53 to 34.75 ± 7.27 g (Fig. 2A, $p < 0.0001$) over 21 days. Constricted rat models also showed significant differences in threshold between ipsilateral and contralateral paws ($p < 0.0001$). PNI triggers enhanced long-term potentiation (LTP) via excitatory synaptic transmission in ACC neurons and exhibits enduring hypersensitivity.

The PWL of the injured hind paw in CCI rats was also altered from 20.39 ± 3.22 to 6.92 ± 2.69 s compared with the PWL of sham controls, 19.46 ± 2.36 to 17.78 ± 2.50 s, (Fig. 2C) in the 21-day period. The injured rats also showed increased thermal sensitivity with a significant decline in thermal latency compared with that of sham controls. Thermal latency in CCI rats decreased from 20. 99 ± 5.72 to 9.08 ± 2.73 s compared with that of sham controls, from 20.73 ± 5.50 to 20.46 ± 2.94 s ($p < 0.0001$), as shown in Fig. 1 and Table 1.

The CCI model encompasses loose ligations on the sciatic nerve with sutures that lead to nerve constriction and swellings. These nerve injury models express boosted responses to mechanical or thermal stimuli called hyperalgesia.

### Optic Inhibition of ACC Improves Behavioral Sensitivity

Subsequent optic fiber implantation and pain behavior tests (mechanical and thermal) under ACC optic stimulation (Fig. 3A) in the moving state were performed. To compare pain behaviors under optic stimulation in each group, ordinary two-way ANOVA was performed followed by Tukey's post hoc test. The CCI rats injected with NpHR virus showed a notable increase in PWT in the yellow light on state (7.05 ± 2.87 g in the pre state, 29.7 ± 3.42 g upon optical stimulation,

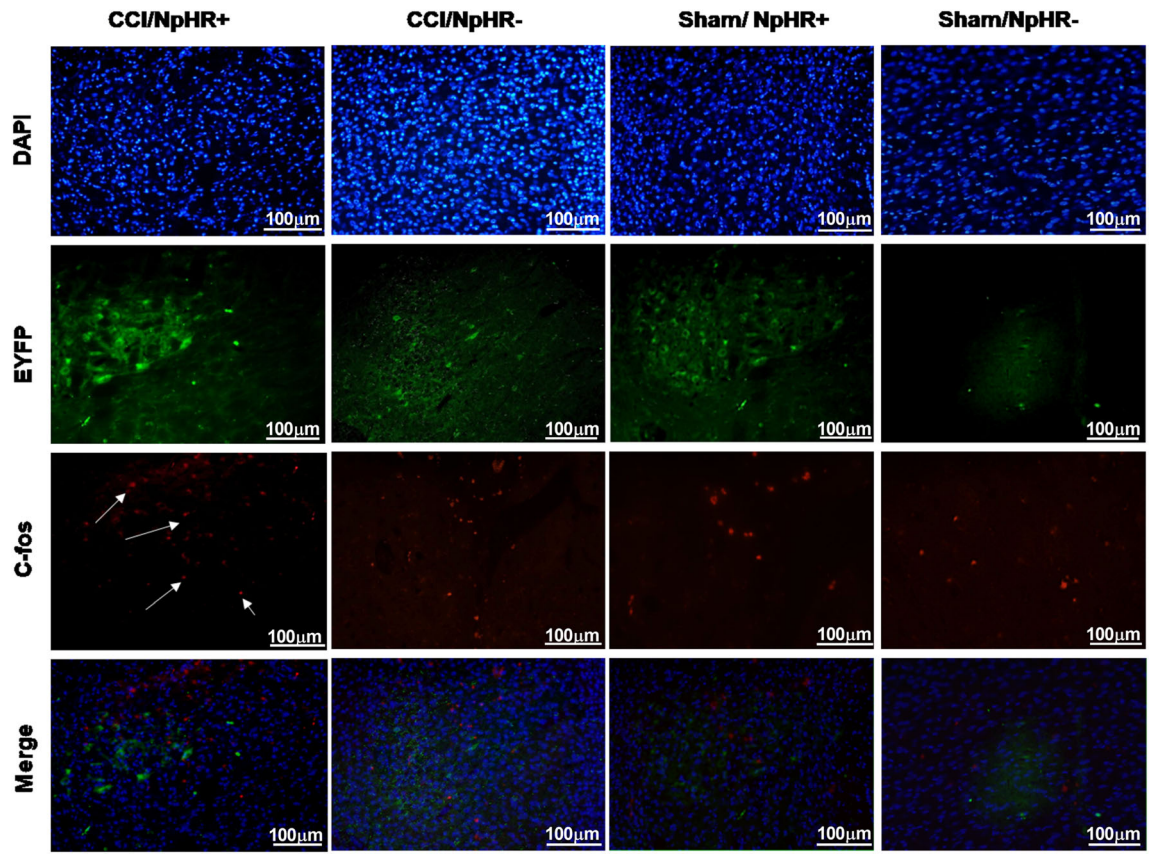


**Fig. 1** Virus expression in the anterior cingulate cortex (ACC). Optogenetic virus and null virus transfection expression of CCI/NpHR+, CCI/NpHR−, Sham/NpHR+, and Sham/NpHR− rats observed by DAPI and EYFP fluorescence. Scale bar = 100 μm. Expression of c-fos in the brain in the ACC indicates the neuronal activation. White arrows show c-fos-positive cells

12.62 ± 4.73 g in the post state, showing statistically significant differences; pre vs. stim, $p$ = 0.0002 and stim vs. post, $p$ = 0.0062). Bonferroni's multiple comparisons was performed following two-way ANOVA to compare CCI with sham controls under optic conditions. Significant differences were observed in light off conditions ($p$ = 0.0005) between the CCI and sham control groups. Likewise, PWL showed improvement in CCI/NpHR+ rats under yellow laser stimulation conditions (5.2 ± 2.67 s in pre, 16.42 ± 4.20 s in stim, and 5.52 ± 1.74 s in post states). Thermal sensitivity decreased in CCI rats in the yellow laser on state, with two-way ANOVA followed by Tukey's multiple comparisons test showing statistical significance between the on and off states. No significant variations were found between pre and post conditions (Table 2).

CCI rats receiving halorhodopsin under optic stimulation (yellow laser) exhibited antinociceptive behavior compared with those receiving the null virus or sham controls. Increased pain sensitivity in the pre and post states in the CCI/NpHR+ group was observed. The halorhodopsin-expressing neurons were triggered by yellow light (~ 590 nm) and underwent hyperpolarization, resulting in neuronal inhibition (Guru et al. 2015); thus, this hyperpolarization leading to inhibition contributes to analgesia. Sham rats injected with halorhodopsin had unchanged behavior during stimulation, thus indicating that ACC optogenetic inhibition responds only under nociception.

## Optogenetic Inhibition of ACC Modulates Neuronal Activity in the VPL Thalamus

To investigate whether ACC inactivation could affect thalamic neurons, in vivo single-unit extracellular recording of ventral posteromedial thalamic neurons was achieved. First, VPL thalamic firing activity was obtained from three rats in each group. Mean firing rates in the VPL thalamus were significantly increased in CCI rats compared with that of sham-operated rats (Fig. 4a and Table 3).

Increased burst firing was identified in the VPL thalamus of CCI/NpHR+ rats compared with that of sham rats and CCI rats injected with the null virus. Burst firing improved significantly with yellow laser stimulation in the ACC, as shown in Fig. 4b. Alterations in thalamic output might vary depending on activation and inhibition of the ACC. We confirmed that modulation of ACC activity using optogenetic techniques in

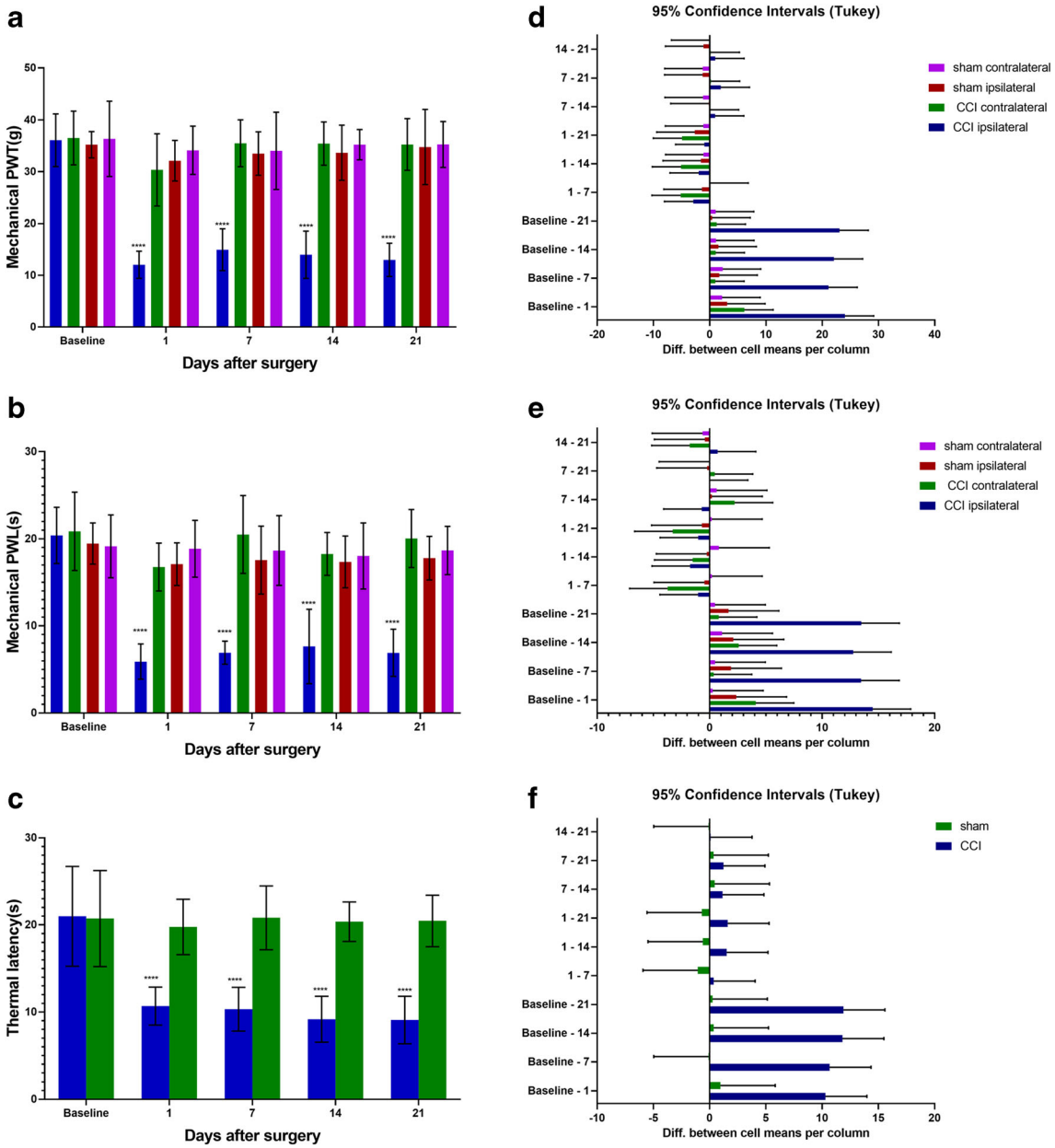


**Fig. 2** Mechanical and thermal sensitivity in response to neuropathic pain. Mechanical (A, B) and thermal (C) thresholds and latencies significantly decreased over time in ipsilateral CCI rat models; the rat model also developed hyperalgesia. D, E, and F show the confidence intervals of panels A, B, and C, respectively. The values are expressed as the mean ± SD. Baseline value = behavior test data before surgery. * represents the significant differences between groups (repeated two-way ANOVA) with Tukey's post hoc multiple comparisons test

CCI rats influenced thalamic output. Optical stimulation of the ACC during yellow laser irradiation decreased thalamic neuronal activity in the NpHR+ group but did not alter activity in the sham controls and CCI/NpHR− groups.

## Discussion

In this study, we used optogenetic inhibition and electrophysiology techniques to investigate the role of the ACC in sciatic nerve CCI-induced neuropathic pain. Behavioral studies indicate that optical inhibition of ACC alleviates PNI-induced neuropathic pain, which parallels previous reports (Chen et al. 2018; Moon et al. 2017). Likewise, in vivo electrophysiological recordings showed hyperactive neuronal activity in the ACC and VPL thalamus in neuropathic pain rat models. Notably, optogenetic inhibition in the ACC resulted in altered sensory thalamic discharge with decreased burst firing.

We observed that inhibition of ACC excitatory neurons increased the mechanical and thermal pain threshold in a

**Table 1** Mechanical and thermal pain sensitivity measured by using a plantar aesthesiometer and hot plate test on sciatic nerve constriction and sham rat models

| Animal groups | Baseline | Day 1 | Day 7 | Day 14 | Day 21 |
|---|---|---|---|---|---|
| Paw withdrawal threshold (in grams) | | | | | |
| CCI ipsilateral | 36.07 ± 5.09 | 12.03 ± 2.62* | 14.95 ± 4.03* | 13.98 ± 4.56* | 12.98 ± 3.22* |
| CCI contralateral | 36.50 ± 5.19 | 30.33 ± 6.99 | 35.48 ± 4.52 | 35.43 ± 4.18 | 35.25 ± 4.98 |
| Sham ipsilateral | 35.20 ± 2.53 | 32.10 ± 3.92 | 33.49 ± 4.20 | 33.65 ± 5.33 | 34.75 ± 7.27 |
| Sham contralateral | 36.34 ± 7.27 | 34.12 ± 4.67 | 34.02 ± 7.46 | 35.21 ± 2.93 | 35.25 ± 4.44 |
| Paw withdrawal latency (in seconds) | | | | | |
| CCI ipsilateral | 20.39 ± 3.22 | 5.90 ± 2.00* | 6.93 ± 1.30* | 7.63 ± 4.26* | 6.92 ± 2.69* |
| CCI contralateral | 20.85 ± 4.48 | 16.76 ± 2.75 | 20.49 ± 4.46 | 18.27 ± 2.46 | 20.04 ± 3.32 |
| Sham ipsilateral | 19.46 ± 2.36 | 17.09 ± 2.44 | 17.55 ± 3.91 | 17.35 ± 2.97 | 17.78 ± 2.50 |
| Sham contralateral | 19.14 ± 3.61 | 18.86 ± 3.27 | 18.66 ± 4.00 | 18.03 ± 3.80 | 18.66 ± 2.77 |
| Thermal latency (in seconds) | | | | | |
| CCI | 20.99 ± 5.72 | 10.69 ± 2.18* | 10.32 ± 2.51* | 9.17 ± 2.63* | 9.08 ± 2.73* |
| Sham | 20.73 ± 5.50 | 19.77 ± 3.17 | 20.82 ± 3.64 | 20.37 ± 2.25 | 20.46 ± 2.94 |

CCI = sciatic nerve–constricted rats ($n = 14$), sham = sham lesioned ($n = 8$). Values are represented as mean ± SD

*$p < 0.0001$ compared with sham and contralateral groups (two-way ANOVA)

**Table 2** Effect of optogenetic inhibition on mechanical and thermal pain sensitivity

| | | Pre | Stim | Post |
|---|---|---|---|---|
| Paw withdrawal threshold (in grams) | | | | |
| CCI/NpHR+ | *ipsi* | 7.05 ± 2.87 | 29.7 ± 3.42* | 12.62 ± 4.73 |
| | *contra* | 32.7 ± 5.58 | 35.75 ± 4.78 | 36.85 ± 4.78 |
| CCI/NpHR− | *ipsi* | 12.95 ± 2.32 | 11.52 ± 4.58 | 12.47 ± 4.16 |
| | *contra* | 37.07 ± 5.01 | 37.45 ± 5.01 | 34.6 ± 5.38 |
| Sham NpHR+ | *ipsi* | 38.85 ± 6.95 | 35.25 ± 2.75 | 32.7 ± 0.2 |
| | *contra* | 37.4 ± 1.7 | 35.75 ± 0.55 | 37.2 ± 2 |
| Sham NpHR− | *ipsi* | 33.05 ± 4.85 | 36 ± 3.5 | 40.8 ± 0.6 |
| | *contra* | 37.4 ± 0.8 | 36 ± 0.8 | 37.8 ± 4.3 |
| Paw withdrawal latency (in seconds) | | | | |
| CCI/NpHR+ | *ipsi* | 5.2 ± 2.67 | 16.42 ± 4.20* | 5.52 ± 1.74 |
| | *contra* | 16.75 ± 3.18 | 17.85 ± 2.44 | 18.02 ± 2.82 |
| CCI/NpHR− | *ipsi* | 6.15 ± 1.90 | 5.92 ± 1.84 | 7.72 ± 1.00 |
| | *contra* | 17.57 ± 3.36 | 18.77 ± 2.51 | 17.35 ± 2.34 |
| Sham NpHR+ | *ipsi* | 20.9 ± 2 | 22.45 ± 3.75 | 19.9 ± 3.7 |
| | *contra* | 18.55 ± 1.25 | 17.35 ± 0.75 | 17.95 ± 1.85 |
| Sham NpHR− | *ipsi* | 18.05 ± 1.65 | 20.8 ± 2.1 | 23.45 ± 2.75 |
| | *contra* | 17.3 ± 0.9 | 18.05 ± 0.85 | 19.45 ± 1.95 |
| Thermal latency (in seconds) | | | | |
| CCI/NpHR+ | | 7.52 ± 1.46 | 15.95 ± 2.08* | 8.17 ± 1.29 |
| CCI/NpHR− | | 8.32 ± 1.14 | 7.9 ± 0.86 | 7.05 ± 1.20 |
| Sham NpHR+ | | 21 ± 2.1 | 20.7 ± 2 | 18.7 ± 1.9 |
| Sham NpHR− | | 22.35 ± 2.55 | 19.65 ± 1.15 | 21.65 ± 0.95 |

CCI/NpHR+ = sciatic nerve–constricted rats receiving halorhodopsin ($n = 4$), CCI/NpHR− = CCI rats receiving null virus ($n = 4$), sham/NpHR+ = sham lesioned receiving halorhodopsin ($n = 2$), sham/NpHR− = sham lesioned receiving null virus ($n = 2$)

*ipsi*, ipsilateral hindpaw; *contra*, contralateral hindpaw

Values are represented as mean ± SD

*$p < 0.0001$ compared with pre and post conditions (two-way ANOVA)

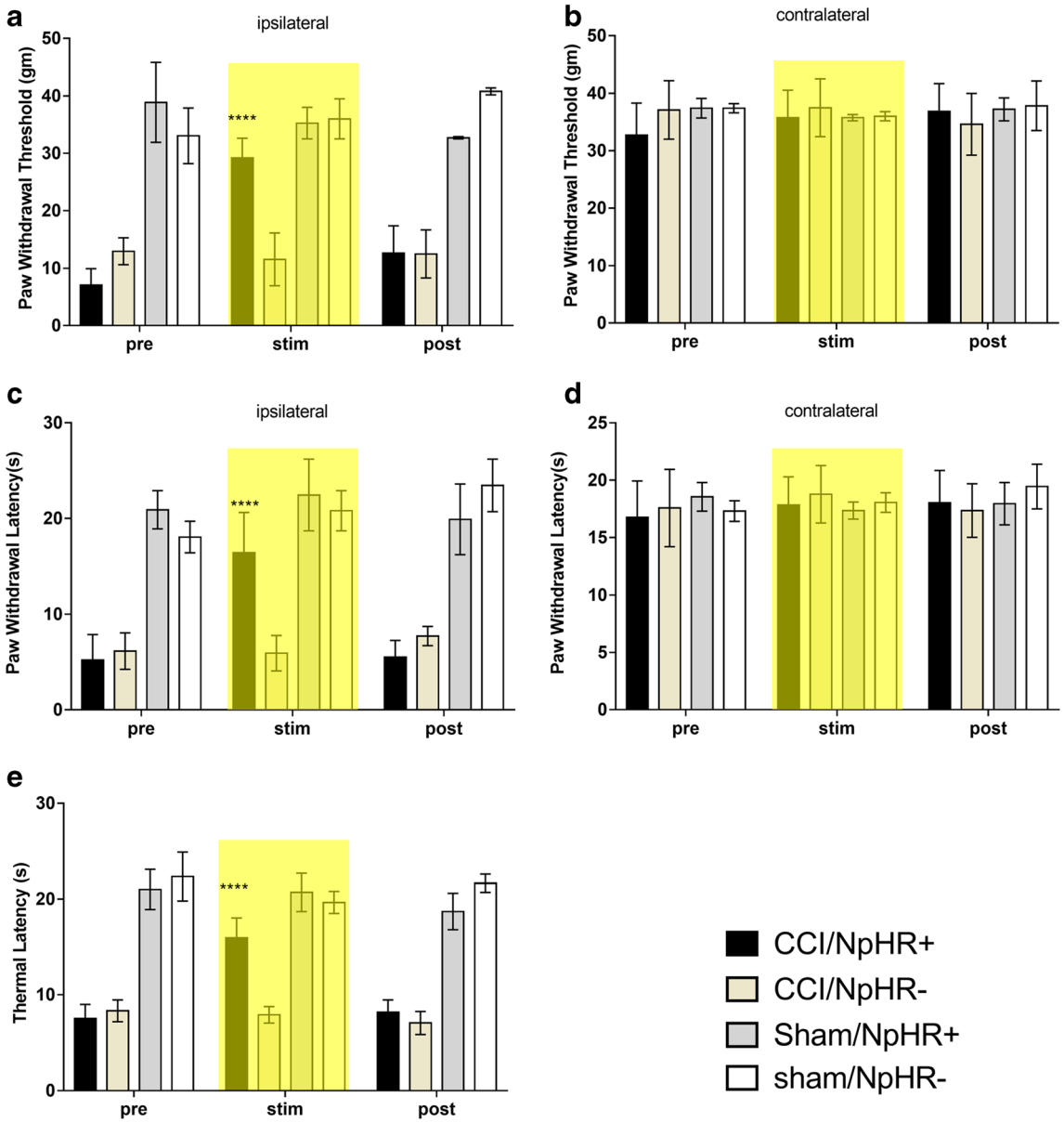


**Fig. 3** Pain sensitivity under different optical conditions. Mechanical (A–D) and thermal (E) pain thresholds and latencies in CCI-NpHr and sham control rats. Yellow shading signifies the laser stimulation period. The yellow laser (595 nm) was adjusted with a waveform generator during mechanical and thermal pain sensitivity tests. The values are expressed as the mean ± SD. * represents the significant differences between groups (repeated two-way ANOVA) with Tukey's post hoc multiple comparisons test

neuropathic pain rat model, which is consistent with previous findings (Chiou et al. 2016; Kang et al. 2015a; Zhuang et al. 2019). Synaptic plasticity along the pain pathway is influenced by changes in the areas of the brain responsible for pain processing and by behavioral variations in PNI-induced neuropathic pain. Previous studies have reported that the ACC is a key region in pain processing (Fuchs et al. 2014b; Xiao and Zhang 2018). The ACC responded to noxious stimuli and was active during pain anticipation (Gu et al. 2015; LaBuda and Fuchs 2005); in addition, endogenous opioid signaling in the ACC has been shown to be essential for pain relief (Navratilova et al. 2015). These responses and functional fast pain modulation are thought to be mediated by the ACC–spinal cord pathway/direct descending projection. The excitatory transmission in layers II/III of the ACC is potentiated after PNI, which may be influenced by both presynaptic and postsynaptic mechanisms (Xu et al. 2008) that exhibit enduring mechanical hypersensitivity. Synaptic potentiation in the ACC and directly in the corticospinal tract may play key roles in pain behavioral hypersensitivity to sensory stimuli in insistent pain conditions (Zhuo 2014b).

The supposed mechanisms of miRNAs in the ACC have been suggested to be related to neuropathic pain induced by CCI of the sciatic nerve (Ding et al. 2018). The increased

**Table 3** Mean firing rate comparison between groups in response to different laser conditions

| Groups and laser conditions | Mean 1 | Mean 2 | *q* | DF | Summary | Adjusted *p* value |
|---|---|---|---|---|---|---|
| CCI/NpHr+ | | | | | | |
| Pre vs. stim—laser on | 15.67 | 6.35 | 9.049 | 24 | **** | < 0.0001 |
| Pre vs. post | 15.67 | 16.96 | 1.249 | 24 | ns | 0.656 |
| Stim—laser on vs. post | 6.35 | 16.96 | 10.3 | 24 | **** | < 0.0001 |
| Sham/NpHR− | | | | | | |
| Pre vs. stim—laser on | 7.93 | 7.58 | 0.3398 | 24 | ns | 0.9687 |
| Pre vs. post | 7.93 | 6.7 | 1.194 | 24 | ns | 0.6796 |
| Stim—laser on vs. post | 7.58 | 6.7 | 0.8545 | 24 | ns | 0.8192 |
| CCI/NpHR− | | | | | | |
| Pre vs. stim—laser on | 17.25 | 15.24 | 1.952 | 24 | ns | 0.3669 |
| Pre vs. post | 17.25 | 16.67 | 0.5632 | 24 | ns | 0.9166 |
| Stim—laser on vs. post | 15.24 | 16.67 | 1.388 | 24 | ns | 0.5951 |
| Sham/NpHR+ | | | | | | |
| Pre vs. stim—laser on | 6.6 | 7.58 | 0.9516 | 24 | ns | 0.7813 |
| Pre vs. post | 6.6 | 9.85 | 3.156 | 24 | ns | 0.0861 |
| Stim—laser on vs. post | 7.58 | 9.85 | 2.204 | 24 | ns | 0.2826 |

CCI/NpHR+ = sciatic nerve–constricted rats receiving halorhodopsin ($n = 3$), CCI/NpHR− = CCI rats receiving null virus ($n = 3$), sham/NpHR+ = sham lesioned receiving halorhodopsin ($n = 3$), sham/NpHR− = sham lesioned receiving null virus ($n = 3$)

****$p < 0.0001$ considered significant (two-way ANOVA with Tukey's multiple comparisons test)

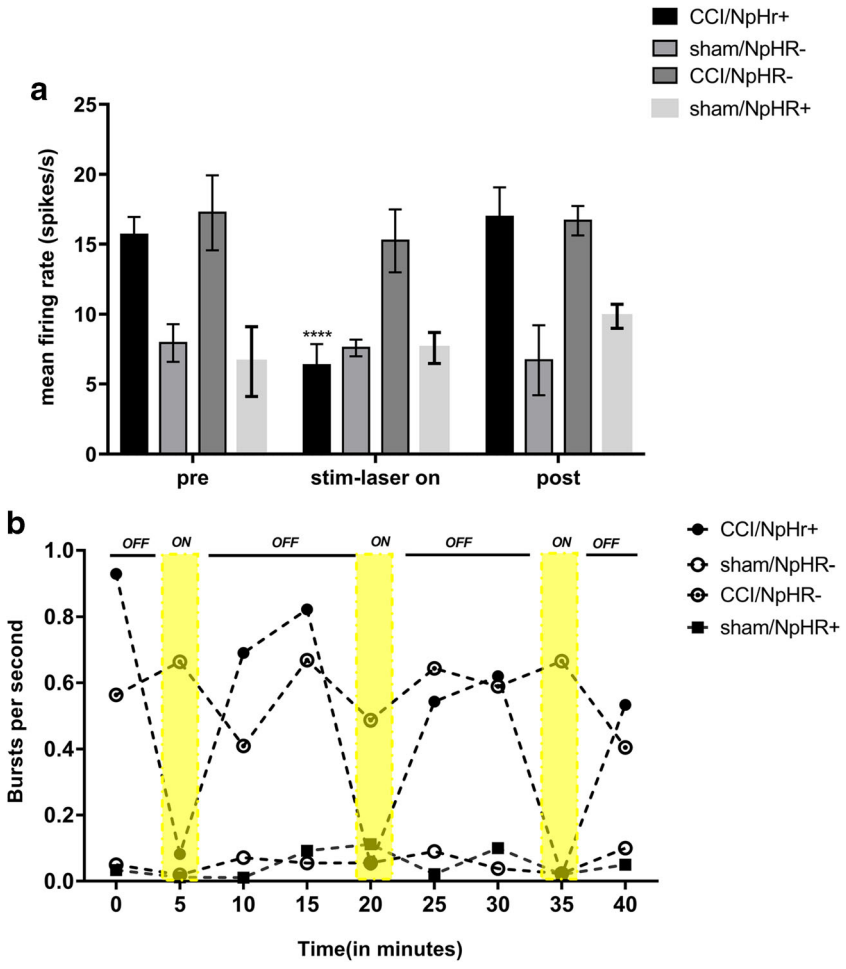


**Fig. 4** In vivo neuronal activity of the VPL thalamus under yellow laser stimulation. **a** Higher mean frequencies were found in CCI/NpHR+ rats than in rats in the NpHR− and sham groups. The firing rate decreased under the yellow laser stimulation condition in CCI/NpHR+ rats, and the firing rate of the other groups was unchanged in all states. **b** VPL thalamic neuron burst firing rate improved with yellow laser stimulation in the ACC in CCI/NpHR+ rats. ON = stimulation period, OFF = stimulation off period

activation of the ACC in both acute and chronic pain situations has been verified with electrophysiological studies. The descending projecting fibers from ACC excitatory neurons are directed to spinal cord dorsal horn laminae III to V. Sensitizing behaviors such as hyperalgesia and allodynia are noted following PNI (Decosterd and Woolf 2000). Moreover, CNS maladaptive changes have been substantiated in neuroimaging studies after PNI (Moisset and Bouhassira 2007; Seifert and Maihöfner 2009). Due to the loss of synaptic inhibition of excitatory pyramidal neurons or increased glutamate release in the ACC, synaptic transmission is escalated, implicating neuronal excitation (Chen et al. 2014) and mechanical hypersensitivity. The disinhibition of ACC layer V pyramidal neurons because of the concentrated amount of GABAergic inhibition has been reported in neuropathic pain animal models. Accordingly, inhibition of synaptic potentiation in the ACC might moderate hypersensitivity. The optogenetic inhibition of calcium/calmodulin-dependent protein kinase II (CaMKII) excitatory neurons in the ACC alleviated mechanical hyperalgesia in inflammatory-induced pain, which reversed suddenly with the termination of light (Kang et al. 2015a; Luo et al. 2008). The ACC is a central cortical area involved in persistent neuropathic pain (Xu et al. 2008) and acts as a positive feedback control system that facilitates spinal nociceptive transmission. A few years ago, it was reported that nerve injury leads to potentiation of the core excitability of pyramidal neurons in ACC; however, the intrinsic excitability potentiation of interneurons was unchanged (Blom et al. 2014b). Thus, an imbalance arises between excitatory and inhibitory somatosensory signaling during PNI in the way that pain signals are tempered in the higher order of the CNS involved in neuropathic pain.

The ACC sustains equilibrium among cortical excitation and inhibition for normal brain function (Gu et al. 2015). The imbalance within neural microcircuitry is related to various diseases and disorders (Yizhar et al. 2011). Most ACC neurons seem to be excitatory, which could possibly inhibit glutamatergic activity in this study. However, instead of a specific glutamatergic promoter, a highly neuron-specific promoter (hSyn) (Kugler et al. 2003) was used in this study. Here, there was a substantial effect on mechanical latency, thermal latency, and the threshold with the optogenetic inhibition of ACC neurons in injured rats. These findings might help support the essential role of excitatory neurons in pain signal transmission. Remarkably, sham controls showed unaltered behavior during optogenetic inhibition of these neurons.

The cingulate cortex is studied as frequently triggered areas in human pain research. Likewise, the thalamus is also frequently activated, and these two structural responses may be correlated. The significant changes include greater spontaneous firing along with periodic bursting patterns in response to stimuli. The ACC directly potentiates spinal sensory transmission, and top-down facilitation promotes chronic neuropathic pain progression. The ACC–spinal cord projecting neurons persuaded behavioral sensitization in pain responses when activated; in contrast, their inhibition eased neuropathic pain. The plasticity alteration in the ACC may enable the transition of nociception from acute to chronic. Electrical stimulation to the medial thalamic nucleus exhibited increased signaling in the ACC, suggesting that the thalamus is involved in the emotional component of pain (Hsu and Shyu 1997; Shyu et al. 2004). PNI triggers plastic changes or LTP in cortical synapses (Zhuo 2006, 2008), which might generate abnormal neuronal spike activity in the brain without obvious peripheral sensory stimulation. VPL thalamic neurons have shown an increased rate of spontaneous firing in in vivo extracellular single-unit activity recordings (Saab 2012). Additionally, increased evoked firing in these neurons is also observed in response to noxious and non-noxious stimuli applied to the hyperalgesic hind paw. We suggest that peripheral neuropathic pain is associated with alterations in ACC and VPL thalamic neuronal activity. Optogenetic inhibition with eNpHr in the ACC caused a reversal effect of abnormal pain behavior as well as bursting patterns in the VPL thalamus. Abnormal thalamic bursting occurs, prompting obstinate nociceptive input from the periphery. These burst firing events may aid in generating increased action potentials in the ACC. In the spinal cord injury rat "central neuropathic pain model," a higher rate of spontaneous firing of VPL thalamic neurons with increased after-discharge has been observed, but VPL thalamic neuron firing conditions in peripheral neuropathic pain have not been well investigated. VPL thalamic electrophysiological changes after sciatic CCI in rats have been studied, and the antinociceptive effects of high-frequency stimulation in VPL thalamic neurons (Iwata et al. 2011) have been verified. Similarly, here, we tried to observe the antinociceptive properties with optical inhibition of the ACC and its influence on VPL thalamic discharge. Our results provide further evidence for a role of ACC in neuropathic pain modulation via optical inhibition. However, this study has some limitations that need to be considered. First, there is a high probability of optogenetic virus transfecting some inhibitory neurons; therefore, their action after optical stimuli could be complex. Spontaneous thalamic discharge can be influenced by anesthetic conditions; however, we tried to avoid spontaneous thalamic discharge with pain provocation in this study. Nonetheless, the observations in this study showed that changes in neuronal activity from the thalamus after optical stimuli could affect pain behavior. In this experiment, the AAV viral vector was used to deliver optogenetic proteins that were more stable and less likely to mutate. However, some cortical area injury is inevitable due to several factors, such as the light source, electrical stimulations, and any other tools; thus, this damage may trigger some unexpected responses. We agree with the notion that had been studied earlier, namely, that rather than descending or ascending pathway

modulation, an alternative approach may be the direct inhibition of hyperactive areas in the brain during neuropathic pain conditions to produce antinociceptive effects (Saab 2012). The combined optogenetic, behavioral, and electrophysiological findings suggest the vital role of the ACC in PNI-induced neuropathic pain and that the ACC serves as a viable target for clinical therapeutics.

In conclusion, neuropathic pain induced by PNI is a devastating neurological state of high clinical significance. Nerve injury causes noteworthy hyperactivity in ACC pyramidal neurons, thus resulting in disinhibition and increased output to the spinothalamic tract through direct or indirect signaling via the brainstem pathway. Hence, the optical inhibition of excited neurons in the ACC affects ventral posterolateral thalamic neuronal activity and contributes to sensory pain relief.

**Authors' Contributions** Conception and design: YSP, ELINA, and HCM. Acquisition of data: ELINA and JAISAN. Analysis and interpretation: HCM and ELINA. Writing article: YSP, ELINA, and HCM. Critical review of article: YSP and HKK. Final approval for publication: YSP. Agreement to be accountable for all aspects of the work: ELINA, HCM, and YSP.

**Funding Information** This work was supported by the National Research Foundation of Korea (NRF 2016H1D5A1908909, NRF 2015H1D3A1066175, NRF 2014K1A3A1A21001372, and NRF 2019R1I1A1A0159554). This work was financially supported by the Research Year of Chungbuk National University in 2018.

## Compliance with Ethical Standards

Animal experiments were performed according to the national guidelines and with approval from the Institutional Animal Care Committee of Chungbuk National University (CBNUR-1072-17).

**Conflict of Interest** The authors declare that they have no conflict of interest.

**Disclaimer** This work was conducted during the 2018–2019 research year at Chungbuk National University.

## References

Bennett GJ, Xie Y-K (1988) A peripheral mononeuropathy in rat that produces disorders of pain sensation like those seen in man. Pain 33:87–107

Blom SM, Pfister J-P, Santello M, Senn W, Nevian T (2014a) Nerve injury-induced neuropathic pain causes disinhibition of the anterior cingulate cortex. J Neurosci 34:5754–5764

Blom SM, Pfister JP, Santello M, Senn W, Nevian T (2014b) Nerve injury-induced neuropathic pain causes disinhibition of the anterior cingulate cortex. J Neurosci 34:5754–5764. https://doi.org/10.1523/JNEUROSCI.3667-13.2014

Cai YQ, Wang W, Hou YY, Pan ZZ (2014) Optogenetic activation of brainstem serotonergic neurons induces persistent pain sensitization. Mol Pain 10:70. https://doi.org/10.1186/1744-8069-10-70

Chen T et al (2014) Postsynaptic potentiation of corticospinal projecting neurons in the anterior cingulate cortex after nerve injury. Mol Pain 10:33

Chen T et al (2018) Top-down descending facilitation of spinal sensory excitatory transmission from the anterior cingulate cortex. Nat Commun 9:1–17

Chiou C-S, Chen C-C, Tsai T-C, Huang C-C, Chou D, Hsu K-S (2016) Alleviating bone cancer–induced mechanical hypersensitivity by inhibiting neuronal activity in the anterior cingulate cortex anesthesiology. J Am Soc Anesthesiol 125:779–792

Daou I, Tuttle AH, Longo G, Wieskopf JS, Bonin RP, Ase AR, Wood JN, de Koninck Y, Ribeiro-da-Silva A, Mogil JS, Seguela P (2013) Remote optogenetic activation and sensitization of pain pathways in freely moving mice. J Neurosci 33:18631–18640

De Vry J, Kuhl E, Franken-Kunkel P, Eckel G (2004) Pharmacological characterization of the chronic constriction injury model of neuropathic pain. Eur J Pharmacol 491:137–148

Decosterd I, Woolf CJ (2000) Spared nerve injury: an animal model of persistent peripheral neuropathic pain. Pain 87:149–158. https://doi.org/10.1016/S0304-3959(00)00276-1

Deuis JR, Vetter I (2016) The thermal probe test: a novel behavioral assay to quantify thermal paw withdrawal thresholds in mice. Temperature (Austin) 3:199–207. https://doi.org/10.1080/23328940.2016.1157668

Ding Z et al (2018) Resveratrol promotes nerve regeneration via activation of p300 acetyltransferase-mediated VEGF signaling in a rat model of sciatic nerve crush injury. Front Neurosci 12:341–341. https://doi.org/10.3389/fnins.2018.00341

Dodla MC, Alvarado-Velez M, Mukhatyar VJ, Bellamkonda RV (2019) Peripheral nerve regeneration. In: Principles of regenerative medicine. Elsevier, pp 1223-1236

Fuchs PN, Peng YB, Boyette-Davis JA, Uhelski ML (2014a) The anterior cingulate cortex and pain processing. Front Integr Neurosci 8:35

Fuchs PN, Peng YB, Boyette-Davis JA, Uhelski ML (2014b) The anterior cingulate cortex and pain processing. Front Integr Neurosci 8:35. https://doi.org/10.3389/fnint.2014.00035

Gage GJ, Kipke DR, Shain W (2012) Whole animal perfusion fixation for rodents. J Visual Exp:JoVE. https://doi.org/10.3791/3564

Gradinaru V, Thompson KR, Deisseroth K (2008) eNpHR: a Natronomonas halorhodopsin enhanced for optogenetic applications. Brain Cell Biol 36:129–139

Gu L, Uhelski ML, Anand S, Romero-Ortega M, Kim YT, Fuchs PN, Mohanty SK (2015) Pain inhibition by optogenetic activation of specific anterior cingulate cortical neurons. PLoS One 10:e0117746. https://doi.org/10.1371/journal.pone.0117746

Guru A, Post RJ, Ho Y-Y, Warden MR (2015) Making sense of optogenetics. Int J Neuropsychopharmacol 18:pyv079. https://doi.org/10.1093/ijnp/pyv079

Harte SE, Spuz CA, Borszcz GS (2011) Functional interaction between medial thalamus and rostral anterior cingulate cortex in the suppression of pain affect. Neuroscience 172:460–473

Hsieh J-C, Stone-Elander S, Ingvar M (1999) Anticipatory coping of pain expressed in the human anterior cingulate cortex: a positron emission tomography study. Neurosci Lett 262:61–64

Hsu MM, Shyu BC (1997) Electrophysiological study of the connection between medial thalamus and anterior cingulate cortex in the rat. Neuroreport 8:2701–2707. https://doi.org/10.1097/00001756-199708180-00013

Huh Y, Bhatt R, Jung D, Shin H-S, Cho J (2012) Interactive responses of a thalamic neuron to formalin induced lasting pain in behaving mice. PLoS One 7:e30699

Hutchison WD, Davis KD, Lozano AM, Tasker RR, Dostrovsky JO (1999) Pain-related neurons in the human cingulate cortex. Nat Neurosci 2:403–405

Im K, Mareninov S, Diaz MFP, Yong WH (2019) An introduction to performing immunofluorescence staining. Methods Molec Biol

(Clifton NJ) 1897:299–311. https://doi.org/10.1007/978-1-4939-8935-5_26

Iwata M, LeBlanc BW, Kadasi LM, Zerah ML, Cosgrove RG, Saab CY (2011) High-frequency stimulation in the ventral posterolateral thalamus reverses electrophysiologic changes and hyperalgesia in a rat model of peripheral neuropathic pain. PAIN 152:2505–2513. https://doi.org/10.1016/j.pain.2011.07.011

Iyer SM et al (2016) Optogenetic and chemogenetic strategies for sustained inhibition of pain. Sci Rep 6:30570

Jagodic MM, Pathirathna S, Joksovic PM, Lee WY, Nelson MT, Naik AK, Su P, Jevtovic-Todorovic V, Todorovic SM (2008) Upregulation of the T-type calcium current in small rat sensory neurons after chronic constrictive injury of the sciatic nerve. J Neurophysiol 99:3151–3156

Kang SJ et al (2015a) Bidirectional modulation of hyperalgesia via the specific control of excitatory and inhibitory neuronal activity in the ACC. Molec Brain 8:81

Kang SJ et al (2015b) Bidirectional modulation of hyperalgesia via the specific control of excitatory and inhibitory neuronal activity in the ACC. Molec Brain 8:1–11

KC E, Moon HC, Kim S, Kim HK, Won SY, Hyun SH, Park YS (2020) Optical modulation on the nucleus accumbens core in the alleviation of neuropathic pain in chronic dorsal root ganglion compression rat model. Neuromodulation 23:167–176

Kim JG, Lim DW, Cho S, Han D, Kim YT (2014) The edible brown seaweed Ecklonia cava reduces hypersensitivity in postoperative and neuropathic pain models in rats. Molecules 19:7669–7678. https://doi.org/10.3390/molecules19067669

Kim KH, Byeon GJ, Kim HY, Baek SH, Shin SW, Koo ST (2015) Mechanical antiallodynic effect of intrathecal nefopam in a rat neuropathic pain model. J Korean Med Sci 30:1189–1196. https://doi.org/10.3346/jkms.2015.30.8.1189

Kugler S, Kilic E, Bahr M (2003) Human synapsin 1 gene promoter confers highly neuron-specific long-term transgene expression from an adenoviral vector in the adult rat brain depending on the transduced area. Gene Ther 10:337–347. https://doi.org/10.1038/sj.gt.3301905

Kügler S, Kilic E, Bähr M (2003) Human synapsin 1 gene promoter confers highly neuron-specific long-term transgene expression from an adenoviral vector in the adult rat brain depending on the transduced area. Gene Ther 10:337–347. https://doi.org/10.1038/sj.gt.3301905

LaBuda CJ, Fuchs PN (2005) Attenuation of negative pain affect produced by unilateral spinal nerve injury in the rat following anterior cingulate cortex activation. Neuroscience 136:311–322

LaGraize SC, Labuda CJ, Rutledge MA, Jackson RL, Fuchs PN (2004) Differential effect of anterior cingulate cortex lesion on mechanical hypersensitivity and escape/avoidance behavior in an animal model of neuropathic pain. Exp Neurol 188:139–148

Lee GH, Kim SS (2016) Therapeutic strategies for neuropathic pain: potential application of pharmacosynthetics and optogenetics. Mediat Inflamm 2016:5808215

Liu J et al (2015) Frequency-selective control of cortical and subcortical networks by central thalamus. Elife 4:e09215

Liu S, Tang Y, Xing Y, Kramer P, Bellinger L, Tao F (2019) Potential application of optogenetic stimulation in the treatment of pain and migraine headache: a perspective from animal studies. Brain Sci 9. https://doi.org/10.3390/brainsci9020026

Luo F, Yang C, Chen Y, Shukla P, Tang L, Wang LX, Wang ZJ (2008) Reversal of chronic inflammatory pain by acute inhibition of Ca2+/calmodulin-dependent protein kinase II. J Pharmacol Exp Ther 325:267–275

McCutcheon JE et al (2014) Optical suppression of drug-evoked phasic dopamine release. Front Neural Circuits 8:114. https://doi.org/10.3389/fncir.2014.00114

Moisset X, Bouhassira D (2007) Brain imaging of neuropathic pain. Neuroimage 37:S80–S88

Moon HC et al (2017) Optical inactivation of the anterior cingulate cortex modulate descending pain pathway in a rat model of trigeminal neuropathic pain created via chronic constriction injury of the infraorbital nerve. J Pain Res 10:2355

Navratilova E et al (2015) Endogenous opioid activity in the anterior cingulate cortex is required for relief of pain. J Neurosci 35:7264–7271. https://doi.org/10.1523/JNEUROSCI.3862-14.2015

Nazeri M, Chamani G, Abareghi F, Mohammadi F, Talebizadeh M-H, Zarei M-R, Shabani M (2019) Sensory and affective dimensions of pain and anxiety like behaviors are altered in an animal model of pain empathy. Iran J Psychiatry 14:221

Nirogi R, Goura V, Shanmuganathan D, Jayarajan P, Abraham R (2012) Comparison of manual and automated filaments for evaluation of neuropathic pain behavior in rats. J Pharmacol Toxicol Methods 66:8–13

Osaka N, Osaka M, Morishita M, Kondo H, Fukuyama H (2004) A word expressing affective pain activates the anterior cingulate cortex in the human brain: an fMRI study. Behav Brain Res 153:123–127

Saab CY (2012) Pain-related changes in the brain: diagnostic and therapeutic potentials. Trends Neurosci 35:629–637

Seifert F, Maihöfner C (2009) Central mechanisms of experimental and chronic neuropathic pain: findings from functional imaging studies. Cell Mol Life Sci 66:375

Shen F-Y et al (2015) Alleviation of neuropathic pain by regulating T-type calcium channels in rat anterior cingulate cortex. Mol Pain 11:s12990-12015-10008-12993

Shevtsova Z, Malik JMI, Michel U, Bähr M, Kügler S (2005) Promoters and serotypes: targeting of adeno-associated virus vectors for gene transfer in the rat central nervous system in vitro and in vivo. Exp Physiol 90:53–59. https://doi.org/10.1113/expphysiol.2004.028159

Shyu BC, Lin CY, Sun JJ, Chen SL, Chang C (2004) BOLD response to direct thalamic stimulation reveals a functional connection between the medial thalamus and the anterior cingulate cortex in the rat. Magn Reson Med 52:47–55. https://doi.org/10.1002/mrm.20111

Sugimine S, Ogino Y, Kawamichi H, Obata H, Saito S (2016) Brain morphological alternation in chronic pain patients with neuropathic characteristics. Mol Pain 12:1744806916652408. https://doi.org/10.1177/1744806916652408

Tachibana K, Kato R, Tsuruga K, Takita K, Hashimoto T, Morimoto Y (2008) Altered synaptic transmission in rat anterior cingulate cortex following peripheral nerve injury. Brain Res 1238:53–58

Wei F, Zhuo M (2008) Activation of Erk in the anterior cingulate cortex during the induction and expression of chronic pain. Mol Pain 4:1744-8069-1744-1728

Xiao X, Zhang YQ (2018) A new perspective on the anterior cingulate cortex and affective pain. Neurosci Biobehav Rev 90:200–211. https://doi.org/10.1016/j.neubiorev.2018.03.022

Xiao Z et al (2019) Cortical pain processing in the rat anterior cingulate cortex and primary somatosensory cortex. Front Cell Neurosci 13:165

Xu H, Wu LJ, Wang H, Zhang X, Vadakkan KI, Kim SS, Steenland HW, Zhuo M (2008) Presynaptic and postsynaptic amplifications of neuropathic pain in the anterior cingulate cortex. J Neurosci 28:7445–7453

Xu L, Liu Y, Sun Y, Li H, Mi W, Jiang Y (2018) Analgesic effects of TLR4/NF-κB signaling pathway inhibition on chronic neuropathic pain in rats following chronic constriction injury of the sciatic nerve. Biomed Pharmacother 107:526–533

Yizhar O et al (2011) Neocortical excitation/inhibition balance in information processing and social dysfunction. Nature 477:171–178. https://doi.org/10.1038/nature10360

Zachariou V, Carr F (2014) Nociception and pain: lessons from optogenetics. Front Behav Neurosci 8:69

Zhao P, Waxman SG, Hains BC (2006) Sodium channel expression in the ventral posterolateral nucleus of the thalamus after peripheral nerve injury. Mol Pain 2:27

Zhao R, Zhou H, Huang L, Xie Z, Wang J, Gan W-B, Yang G (2018) Neuropathic pain causes pyramidal neuronal hyperactivity in the anterior cingulate cortex. Front Cell Neurosci 12:107

Zhuang X et al. (2019) The anterior cingulate cortex projection to the dorsomedial striatum modulates hyperalgesia in a chronic constriction injury mouse model. Arch Med Sci 15

Zhuo M (2006) Molecular mechanisms of pain in the anterior cingulate cortex. J Neurosci Res 84:927–933

Zhuo M (2008) Cortical excitation and chronic pain. Trends Neurosci 31: 199–207

Zhuo M (2014a) Long-term potentiation in the anterior cingulate cortex and chronic pain. Philosoph Transact R Soc B: Biol Sci 369: 20130146

Zhuo M (2014b) Long-term potentiation in the anterior cingulate cortex and chronic pain. Philos Trans R Soc Lond Ser B Biol Sci 369: 20130146. https://doi.org/10.1098/rstb.2013.0146

Zimmermann M (1986) Ethical considerations in relation to pain in animal experimentation. Acta Physiol Scand Suppl 554:221–233